


## RESEARCH ARTICLE

**A $\beta$  oligomers trigger and accelerate A $\beta$  seeding**

Natalie Katzmarski<sup>1,2,3</sup>; Stephanie Ziegler-Waldkirch<sup>1,2,3</sup>; Nina Scheffler<sup>1,3</sup>; Christian Witt<sup>1,3</sup>; Claudia Abou-Ajram<sup>4</sup>; Brigitte Nuscher<sup>4</sup>; Marco Prinz<sup>2,5,6</sup>; Christian Haass<sup>4,7,8</sup>; Melanie Meyer-Luehmann<sup>1,2,\*</sup> 

<sup>1</sup> Department of Neurology, Medical Center – University of Freiburg, Freiburg, Germany.

<sup>2</sup> Faculty of Medicine, University of Freiburg, Freiburg, Germany.

<sup>3</sup> Faculty of Biology, University of Freiburg, Freiburg, Germany.

<sup>4</sup> Biomedical Center (BMC), Ludwig-Maximilians-University Munich, Munich, Germany.

<sup>5</sup> Institute of Neuropathology, Medical Center – University of Freiburg, Freiburg, Germany.

<sup>6</sup> BIOS Centre for Biological Signalling Studies, University of Freiburg, Freiburg, Germany.

<sup>7</sup> German Center for Neurodegenerative Diseases (DZNE), Munich, Germany.

<sup>8</sup> Munich Cluster for Systems Neurology (SyNergy), Munich, Germany.

**Keywords**

Alzheimer's disease, A $\beta$  seeding, A $\beta$  oligomers, amyloid- $\beta$  plaques.

**Abbreviations**

A $\beta$ , amyloid- $\beta$ ; AD, Alzheimer's disease; APP, amyloid precursor protein; CSF, cerebrospinal fluid; DCX, doublecortin.

**Corresponding author:**

Melanie Meyer-Luehmann, PhD,  
Neurocenter, University of Freiburg,  
Breisacher Str.64, 79106 Freiburg, Germany  
(E-mail: [melanie.meyer-luehmann@uniklinik-freiburg.de](mailto:melanie.meyer-luehmann@uniklinik-freiburg.de))

Received 20 February 2019

Accepted 6 May 2019

Published Online Article Accepted

17 May 2019

doi:10.1111/bpa.12734

**Abstract**

Aggregation of amyloid- $\beta$  (A $\beta$ ) that leads to the formation of plaques in Alzheimer's disease (AD) occurs through the stepwise formation of oligomers and fibrils. An earlier onset of aggregation is obtained upon intracerebral injection of A $\beta$ -containing brain homogenate into human APP transgenic mice that follows a prion-like seeding mechanism. Immunoprecipitation of these brain extracts with anti-A $\beta$  oligomer antibodies or passive immunization of the recipient animals abrogated the observed seeding activity, although induced A $\beta$  deposition was still evident. Here, we establish that, together with A $\beta$  monomers, A $\beta$  oligomers trigger the initial phase of A $\beta$  seeding and that the depletion of oligomeric A $\beta$  delays the aggregation process, leading to a transient reduction of seed-induced A $\beta$  deposits. This work extends the current knowledge about the role of A $\beta$  oligomers beyond its cytotoxic nature by pointing to a role in the initiation of A $\beta$  aggregation *in vivo*. We conclude that A $\beta$  oligomers are important for the early initiation phase of the seeding process.

**INTRODUCTION**

Misfolding and aggregation of certain proteins are fundamental features of neurodegenerative diseases. In AD, genetic evidence from mutations in the amyloid precursor protein (APP) and Presenilins strongly implicate A $\beta$  in the pathogenesis of familial AD (4, 10). Fibrillogenesis from A $\beta$  monomers to oligomers, protofibrils and finally fibrils occurs via a nucleation dependent polymerization process. This cascade of A $\beta$  aggregation can also be induced *in vivo* by a single inoculation of A $\beta$ -rich brain extract in mouse models of cerebral amyloidosis that follows a prion-like seeding mechanism (12, 20). The spreading of A $\beta$  pathology to other brain regions originates within the limbic connectome (35) and is thought to involve the transport of preformed A $\beta$  aggregates that nucleate the formation of new amyloid deposits (11), suggesting an involvement of A $\beta$  in the seeding process. There is a growing evidence that aggregated A $\beta$  in the brain homogenate is essential for the amyloid-inducing activity.

Both, aggregate depletion of these brain extracts as well as immunizing the recipient-seeded mice with an anti-A $\beta$  antibody prevented seeding (6, 20, 21), while synthetic A $\beta$  preparations accelerated A $\beta$  pathology but seemed to be less potent compared to complete brain homogenate (29). The amyloid-inducing agent was shown to range in size from small, soluble to proteinase K-resistant assemblies (15). Extended sonification of the brain extract increased the seeding capacity (15), whereas treatment with formaldehyde or boiling reduced the seeding potential (8, 20).

Although many features of the seed-inducing factor have been uncovered in the past, the role of A $\beta$  intermediates, in particular of oligomers, during seeding remains elusive. There is mounting evidence that oligomers are not only the most neurotoxic form of A $\beta$  (14, 31, 34) but also an important intermediate form that might itself play a role in the aggregation process. Injection of A $\beta$  oligomers into the lateral ventricle of nonhuman primates induced AD-like pathology

such as tau hyperphosphorylation or synaptic loss and accumulated in brain regions associated with memory and cognitive functions (7). Since passive immunization with antibodies against A $\beta$  oligomers resulted in a reduction of plaque burden and an improvement of cognitive functions in APP transgenic mice (16, 27, 28), we further investigated the ability of oligomeric A $\beta$  to influence the seeding process.

## MATERIAL AND METHODS

### Mice

We used heterozygous 5 $\times$ FAD transgenic mice coexpressing human APP<sup>K670N/M671L</sup> (Sw)+I716V (Fl)+V717I(Lo) and PS1<sup>M146L+L286V</sup> under the control of the neuron-specific Thy-1 promoter (23) and heterozygous APP23 transgenic mice (30) expressing human APP<sup>K670N/M671L</sup>. We backcrossed heterozygous 5 $\times$ FAD and APP23 mice to C57BL/6N mice to generate heterozygous 5 $\times$ FAD or APP23 mice and non-transgenic littermates. Animals were group-housed under specific pathogen-free conditions. Mice were kept under a 12-h light, 12-h dark cycle with food and water *ad libitum*. All animal experiments were carried out in accordance with the policies of the state of Baden-Württemberg under license numbers G13-093 and G16-60.

### Preparation of brain extract for intracerebral injections

Brains from aged (5 $\times$ FAD 51-week-old/APP23 84-week old) amyloid-depositing transgenic mice or young 5 $\times$ FAD mice (14-week old) were used. After removal of the cerebellum, the brain samples were immediately fresh frozen on dry ice and stored at  $-80^{\circ}\text{C}$  until use. Samples were homogenized at 10% (w/v) in sterile phosphate-buffered saline (PBS, Lonza), sonicated  $3 \times 5$  s (70% amplitude) and centrifuged at 3000 g for 5 minutes. The supernatant was stored until use at  $-80^{\circ}\text{C}$ .

### Immunoprecipitation of brain extract

For immunoprecipitation (IP), 400  $\mu\text{g}$  of total protein from brain extract (10% w/v) was diluted in a total volume of 1000  $\mu\text{L}$ . G sepharose beads (GE Healthcare) were washed  $3 \times$  with PBS and 50  $\mu\text{L}$  per 500- $\mu\text{L}$  diluted brain homogenate were incubated with 1  $\mu\text{L}$  of A $\beta$  antibody 3552 (kindly provided by E. Kremmer, Ludwig Maximilians University, Munich, Germany) (33) or amyloid oligomeric-specific antibody A11 (A11, Millipore) overnight by  $4^{\circ}\text{C}$  shaking head over heel. The supernatant was reused. This experiment was repeated until the remaining oligomers resulted in greatly reduced band intensities as detected by western blot probed with A $\beta$  antibody 6E10 (Covance). The cleared supernatant was used for the experiments.

### CSF collection

CSF samples were taken as described previously, with slight modification (1, 5). CSF samples were taken from

the cisterna magna of anesthetized mice using glass micropipettes (Stoelting). Samples were checked for blood contamination by visual examination, and those with blood contamination were excluded from the analysis. The samples were frozen immediately at  $-80^{\circ}\text{C}$ .

### Stereotaxic surgery

Mice were anesthetized via intraperitoneal injection of a mixture of ketamine (100 mg/kg body weight) and xylazine (10 mg/kg body weight) in saline. For bilateral stereotaxic injections of brain homogenates, a Hamilton syringe needle was placed into the hippocampus (AP-2.3 mm; lateral  $\pm 2.0$  mm; DV 2.0 mm) of 6-week-old male 5 $\times$ FAD mice or 24-week-old male APP23 mice. A volume of 2.0  $\mu\text{L}$  (or as indicated) was injected at an injection speed of 1.25  $\mu\text{L}/\text{min}$  and the needle was kept in place for additional 2 minutes before withdrawal. The surgical site was cleaned with sterile saline and the incision sutured. Mice were monitored until recovery from anesthesia.

### Passive immunization

For passive immunization 6-week-old male 5 $\times$ FAD mice were stereotactically injected with 10% w/v aged brain homogenate. The weekly antibody treatment with either 100  $\mu\text{L}$  of amyloid oligomeric antibody A11 (Millipore) or with 100- $\mu\text{L}$  rabbit IgG as control, started 2 weeks after stereotaxic injections of brain homogenates. Mice were sacrificed 1 week after the last treatment.

### Histology

Mice were deeply anesthetized with a mixture of ketamine (300 mg per kg) and xylazine (20 mg per kg) and transcardially perfused with ice-cold PBS and 4% paraformaldehyde. Brains were removed and postfixed for 24 h in 4% paraformaldehyde (Roti<sup>®</sup>-Histofix, Roth), followed by 48 h in 30% sucrose (in PBS). Frozen brains were cut into 25- $\mu\text{m}$ -thick coronal serial sections on a sliding microtome (SM2000R, Leica Biosystems, Wetzlar, Germany) and collected in 5% Glycerol (in PBS). Immunofluorescence staining was performed using the following antibodies: rabbit polyclonal antibody 3552 specific for A $\beta$  1-40 (kindly provided by E. Kremmer, Ludwig Maximilians University, Munich, Germany; diluted 1:3000), rabbit anti-doublecortin (DCX; 1:5000; abcam), mouse monoclonal anti-NeuN (1:200; Millipore) and DAPI (Roche) was used as a counterstain. Dense-core plaques were stained with Thiazine Red (Sigma Aldrich; 2  $\mu\text{M}$  solution in PBS for 5 minutes at RT followed by  $3 \times 5$  minutes washes). Appropriate secondary antibodies conjugated to Alexa 488 or 555 (1:1500) were used.

### Assessment of A $\beta$ plaque load and cell analysis

Fluorescent images of brain slices were taken using a Zeiss Axio Imager M2M microscope with a CCD camera. Every 10th brain section was immunostained and A $\beta$  load was

determined as a fraction of the hippocampus immunoreactive for A $\beta$  using the imaging software ImageJ (National Institutes of Health freeware). Cell number was quantified by counting the number of immunoreactive cells for DCX in the dentate gyrus in a 1 in 10 series of sections throughout the whole hippocampus; three to five animals per group and six sections per animal were analyzed. The hippocampal area was defined based on the mouse brain atlas (26). All analyses were conducted in a blinded manner. Confocal images of NeuN-positive cells in the dentate gyrus were taken with an Olympus confocal microscope (Fluoview FV 1000).

### Quantification of A $\beta$ by immunoassay

Human A $\beta$  was measured by a sandwich electrochemiluminescence (ECL)-linked immunoassay using the Meso Scale Discovery Sector Imager 2400, as described previously (24). For more sensitive detection of A $\beta$  species, the MSD Triplex sandwich immunoassay was used (25). All samples were measured in duplicates.

### Immunoblot analysis of injected brain homogenates and CSF

CSF and Brain homogenates used for injection and immunoprecipitation were subjected to SDS-PAGE using 10%–20% Tris-tricine gels (Invitrogen). Proteins were transferred onto a nitrocellulose membrane (0.1- $\mu$ m pore size; Protran; Whatman) and probed with antibodies specific to human A $\beta$  (6E10, Covance, 1:2000 dilution), and (3552; 1:2000 dilution) or with an antibody specific to oligomers (A11, Millipore, 1:1000 dilution) and visualized using Amersham ECL plus (GE Healthcare).

### Dot blot assay

Two microliters of each sample were transferred onto a nitrocellulose membrane (0.1- $\mu$ m pore size; Whatman). Membranes were allowed to air dry and subsequently immunoblotted using antibodies 6E10 and A11 and corresponding HRP-conjugated secondary antibodies. Antibody reactivity was visualized using the ECL reagent. Bioluminescence was assessed in a Chemidoc MP imaging system (Bio-Rad, Munich, Germany).

### Statistical analysis

Data sets were tested for normality with the Kolmogorov–Smirnov test and the appropriate parametric or non-parametric statistical comparison test was carried out using GraphPad Prism software, version 6.2. Depending on the outcome, the test used was either parametric or non-parametric, i.e. one-way ANOVA or the Kruskal–Wallis test, the *t* test or Mann–Whitney test. Significance level  $\alpha$  was set at 0.05. Reported values are means  $\pm$  S.E.M.

## RESULTS

### Depletion of A $\beta$ oligomers delays the initiation of exogenously induced amyloidosis

We used an indirect approach and injected 6-week-old pre-depositing 5 $\times$ FAD mice (23) with A $\beta$ -containing brain homogenate (10% w/v) followed by weekly treatment with either the oligomer-specific antibody A11 (13) or a polyclonal IgG serum as control to determine the role of A $\beta$  oligomers in the seed-induced A $\beta$  plaque development (Figure 1A). This passive immunization treatment regimen significantly reduced the seed-induced plaque load, although amyloid induction was still observed and not completely abolished (Figure 1B). In an alternative approach, we injected 5 $\times$ FAD mice either with A $\beta$ -containing brain homogenate from aged 5 $\times$ FAD mice, with brain homogenate immunodepleted with A11 for A $\beta$  oligomers or with brain homogenate immunodepleted for A $\beta$ . Immunoblotting and dot blot assays confirmed the presence of total protein and monomeric A $\beta$  in both inoculates but significantly less oligomeric A $\beta$  in the A11 immunodepleted extract and almost no oligomeric and monomeric A $\beta$  in the A $\beta$ -immunodepleted extract (Figure 1C). Again, quantification of A $\beta$  immunoreactivity revealed that the A11-immunodepleted extract yielded a significantly less induced A $\beta$  deposition than the complete brain homogenate, whereas the uninjected or wt injected 5 $\times$ FAD controls at the same age were free of A $\beta$  deposits (Figure 1D). Similar findings were obtained when we injected APP23 mice (30) with aged APP23 transgenic brain extract or its immunodepleted versions (Figure 1E,F), suggesting that the almost complete absence of oligomeric A $\beta$  intermediates limits A $\beta$  seeding.

### Time course of A $\beta$ seeding

Since seeding was shown to be a time-dependent process (20), we next performed a time course analysis. The first seeded A $\beta$  plaques were observed 6 weeks post-injection in 80% of 5 $\times$ FAD mice that had been injected with complete brain extract but were mostly absent in the ones injected with immunodepleted brain extract (Figure 2A, C and E) and completely absent in uninjected 5 $\times$ FAD mice of the same age (Supplementary Figure 1A,B), indicating that the lack of A $\beta$  oligomers in the inoculate delays the onset of seeding. Interestingly, at longer incubation times, the formerly significant difference in the amount of seeding was diminished and disappeared over time (Figure 2A,C). The same phenomenon was observed in APP23 transgenic mice (Figure 2B,C). To account for the differences in the amount of total A $\beta$  in the brain extract measured by ELISA (5 $\times$ FAD: ratio complete/A $\beta$  oligomer IP: 4.5; APP23: ratio complete/A $\beta$  oligomer IP: 3), we adjusted the volumes of the A11-immunodepleted brain extract accordingly. However, this adjustment neither changed the amount of induced A $\beta$  deposits (Figure 2D) nor did it reach the same percentage of visible seeding pattern (complete brain homogenate: 80% vs. increased volume of A $\beta$  oligomer IP: 40%) at 6 weeks



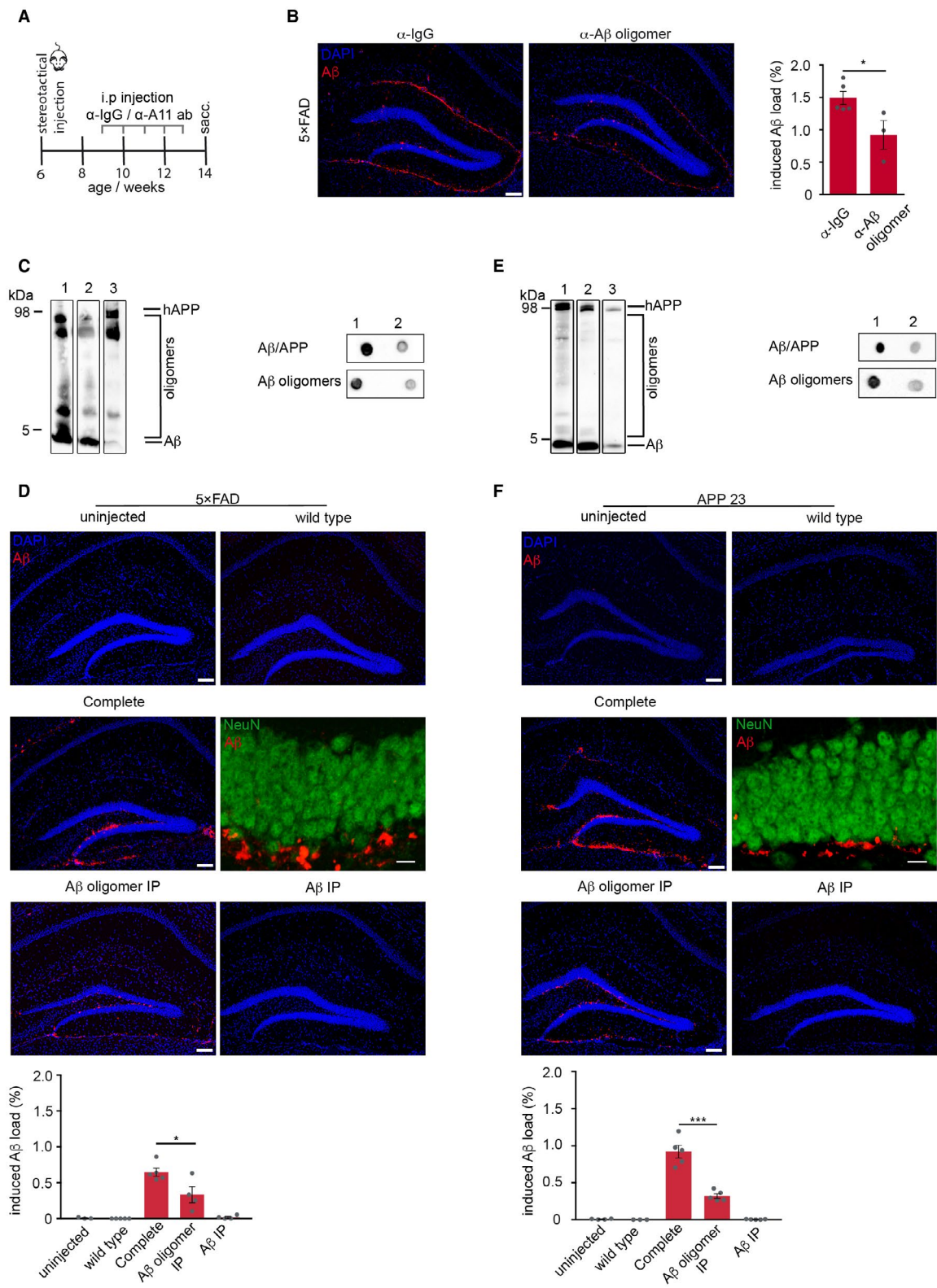


**Figure 1.** Reduction of A $\beta$  oligomers diminishes exogenously induced A $\beta$  deposition. **A.** Schematic representation of the passive immunization paradigm. 6-week-old 5 $\times$ FAD transgenic mice were intracerebrally injected with A $\beta$ -containing brain homogenate (10% w/v) from aged mice, followed by weekly intraperitoneal administration of either A11 antibody or IgG for 5 weeks. **B.** Immunofluorescence staining against A $\beta$  with antibody 3552 (red) and quantification of hippocampal-induced A $\beta$  load revealed significantly reduced A $\beta$  load in mice passively immunized with A11 antibody compared to control immunized mice with IgG ( $n = 3$ –5 mice per group) Mann–Whitney test:  $*P = 0.036$ . **C.** Immunoblot analysis with A $\beta$ -specific antibody 6E10 of brain homogenate from 5 $\times$ FAD that was used for injections. **D.** Reduction of A $\beta$  oligomers in the injected brain homogenate significantly reduced seed-induced A $\beta$  deposition in 5 $\times$ FAD tg mice. **E.** Immunoblot analysis with A $\beta$ -specific antibody 6E10 of brain homogenate from APP23

transgenic mice that was used for injections. Note that A $\beta$  oligomers were significantly reduced in the aged brain homogenate after several rounds of immunoprecipitation with A11 antibody (lane 2) and total A $\beta$  after immunoprecipitation with antibody 3552 (lane 3). Representative dot blots confirmed the low abundance of total A $\beta$ /APP and A $\beta$  oligomers in the A11-depleted brain homogenate. **F.** Reduction of A $\beta$  oligomers in the injected brain homogenate significantly reduced seed-induced A $\beta$  deposition in APP23 mice. Injection of wt brain homogenate or A $\beta$ -depleted brain homogenate failed to induce seeding in 5 $\times$ FAD and APP23 transgenic mice. Confocal images of NeuN-positive neurons (green) and A $\beta$  (red) confirm that the seed-induced A $\beta$  deposits are located extracellularly. Unpaired  $t$ -test for 5 $\times$ FAD mice ( $n = 4$ –5 mice per group):  $*P = 0.03$  and for APP23:  $***P = 0.0002$ . Scale bar in (B, D and F) indicates 100  $\mu$ m in the overview and 10  $\mu$ m in the higher magnification images in (D and F).

post-injection (Figure 2E). Thus, larger volumes of A11-immunodepleted brain homogenate failed to accelerate A $\beta$  seeding.

### Seeding capacity of A $\beta$ oligomers in CSF and young brain homogenate

Previous studies have proposed A $\beta$  peptides, in particular soluble forms of A $\beta$  as seeding factor (6, 15, 20, 29), but the exact A $\beta$  seeding species still remains elusive. In order to circumvent the use of artificial synthetic assemblies, we focused on the cerebrospinal fluid (CSF) and brain homogenate of young APP transgenic mice (19) as natural sources for A $\beta$  oligomers and assessed their potencies to seed A $\beta$  plaques. We found excessive amounts of A $\beta$  oligomers but only negligible monomeric A $\beta$  in both preparations and especially in CSF (Figures 3A,C and 4A). However, despite the high abundance of A $\beta$  oligomers in both inoculates, no seeded plaques were observed even when the injection volumes were doubled (Figures 3B,D and 4B), indicating that oligomeric A $\beta$  alone fails to induce seeding, thus implying the importance of concomitant monomeric A $\beta$  bioavailability.

### Spreading of induced A $\beta$ deposits is independent of A $\beta$ oligomers and has no effect on newborn neurons

Since exogenously induced cerebral  $\beta$ -amyloidosis in APP transgenic mice was shown to spread within the limbic connectome and use neuronal pathways (35), we next compared the efficiency of complete vs. A11-immunodepleted brain homogenate to induce A $\beta$  spreading and the ability to induce dense-core plaques. To address this question, we first analyzed the emergence of A $\beta$  deposits in the dorsal subiculum and entorhinal cortex of 5 $\times$ FAD mice that had been inoculated with A $\beta$  seeds into the hippocampal formation. After 10 weeks of incubation, the amount of amyloid induction was remarkably similar and was not significantly different between both injection groups in the subiculum as well as in the entorhinal cortex (Supplementary Figure

2A). This was also true for the number of seeded Thiazine Red-positive dense-core plaques in the hippocampus (Supplementary Figure 2B), suggesting that the formation of compact plaques was independent of the presence of A11-reactive oligomers in the inoculant.

Due to the cytotoxicity of A $\beta$  oligomers (32), we finally assessed the impact of A11-reactive oligomers in the inoculate on newborn neurons and examined the number of DCX-positive cells at 2, 8 and 10 weeks post-injection. As expected, we found a reduction of DCX-positive cells over time (36), but there was no significant difference between the two brain homogenate preparations (Supplementary Figure 3), which is consistent with a recent publication describing little or no cytotoxic activity of high molecular weight oligomers (34).

## DISCUSSION

In summary, we here report the importance of A $\beta$  oligomers for the early and rapid seed-induced aggregation process as they represent the first nucleation step in the absence of A $\beta$  fibrils. As soon as fibrils are formed in the diseased brain, further additional aggregation and the growth of A $\beta$  deposits follows a pathway independent of A11-reactive oligomers. The formation of these oligomers could therefore be determined as the time-limiting step. In the present study, a significant reduction of these A11 oligomers in the brain homogenate and the immunization with A11 antibody-limited A $\beta$  seeding and was shown to influence the initial step of the A $\beta$  polymerization process by delaying the development of seed-induced A $\beta$  plaques. However, A11-depleted brain homogenate retained its seeding capacity, although to a lesser extent, suggesting that the remaining monomers are sufficient to induce A $\beta$  deposition. However, due to our immunoprecipitation procedure, we can't rule out completely that A $\beta$  fibrils might play a role as well. Interestingly, with longer incubation times, this difference in the amount of seeding disappeared over time indicating that once aggregation starts, A $\beta$  oligomers might only play a minor role during the later aggregation



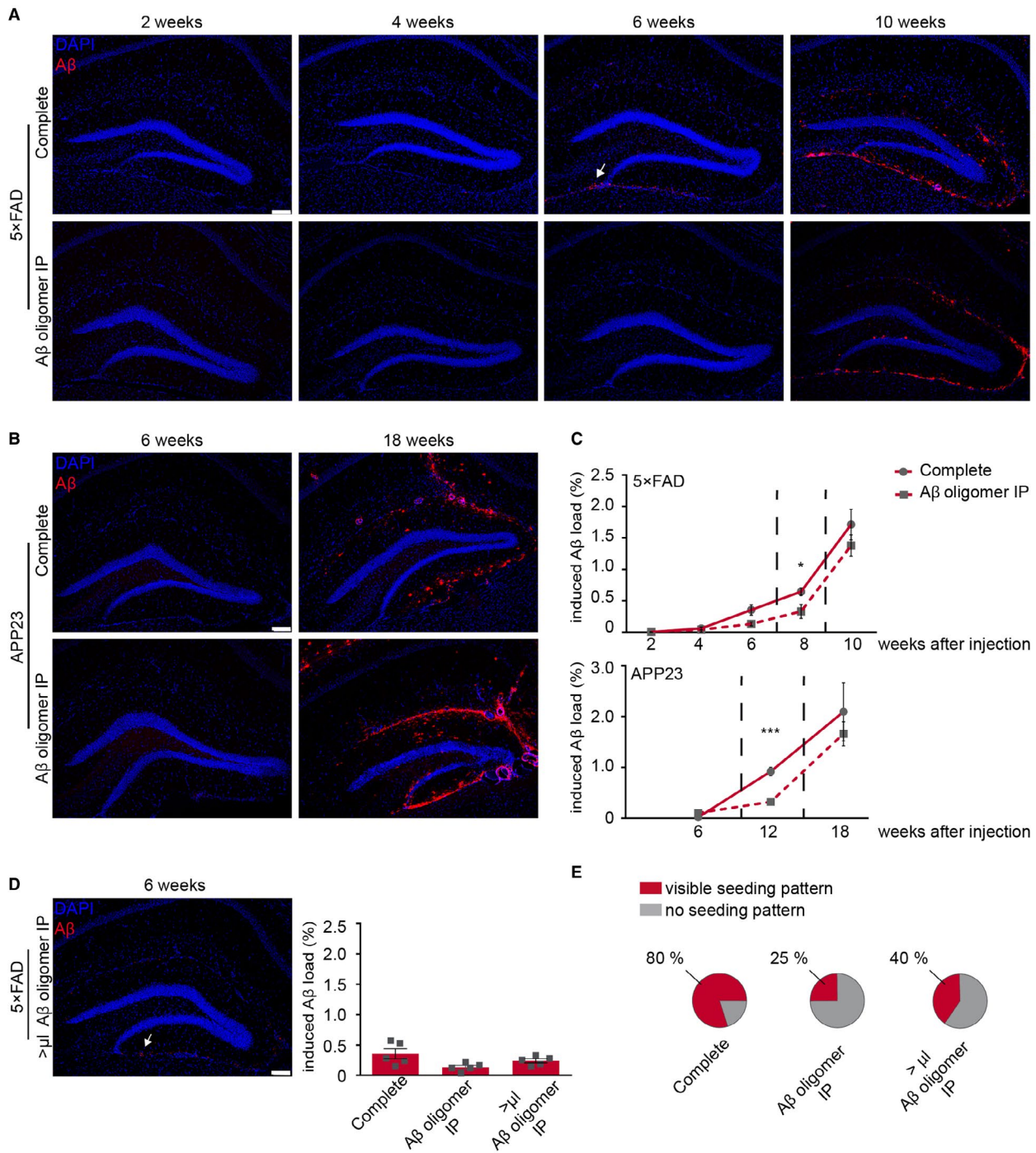


**Figure 2.** Seed-induced A $\beta$  load aligns with longer incubation time. **A.** 6-week-old 5x FAD transgenic mice were injected with complete brain homogenate or A $\beta$  oligomer depleted brain homogenate and incubated for 2, 4, 6 or 10 weeks. First seed-induced A $\beta$  deposits appeared at 6 weeks post-injection in mice injected with complete brain homogenate (white arrow). **B.** 24-week-old APP23 transgenic mice were injected with complete brain homogenate or A $\beta$  oligomer-depleted brain homogenate and incubated for 6 or 18 weeks. **C.** The induced A $\beta$  load was nearly similar 10 weeks after injection in 5x FAD mice (upper graph) and was not significantly different 18 weeks after injection in APP23 mice (lower graph). The cohort of mice for the 8-week time point is

reused from Figure 1D,F as indicated by the dashed lines. **D.** The injection of a higher volume (>1  $\mu$ L) of A11-depleted brain homogenate shows an earlier onset of induced A $\beta$  deposition (white arrow) and a slight but not significant increase at 6 weeks post-injection ( $n = 5$  mice per group; One-way ANOVA:  $F(2,12) = 2.495$   $P = 0.1241$ ; n.s.; Tukey's multiple comparisons test n.s.). **E.** In 80% of 5x FAD injected with complete brain homogenate a typical seeding pattern was visible compared to only 25% when A11-depleted homogenate was injected and 40% when a higher volume (>1  $\mu$ L) of the latter brain homogenate was intracerebrally injected. Scale bar in (A, B and D) represents 100  $\mu$ m. Indicated is the mean  $\pm$  S.E.M.

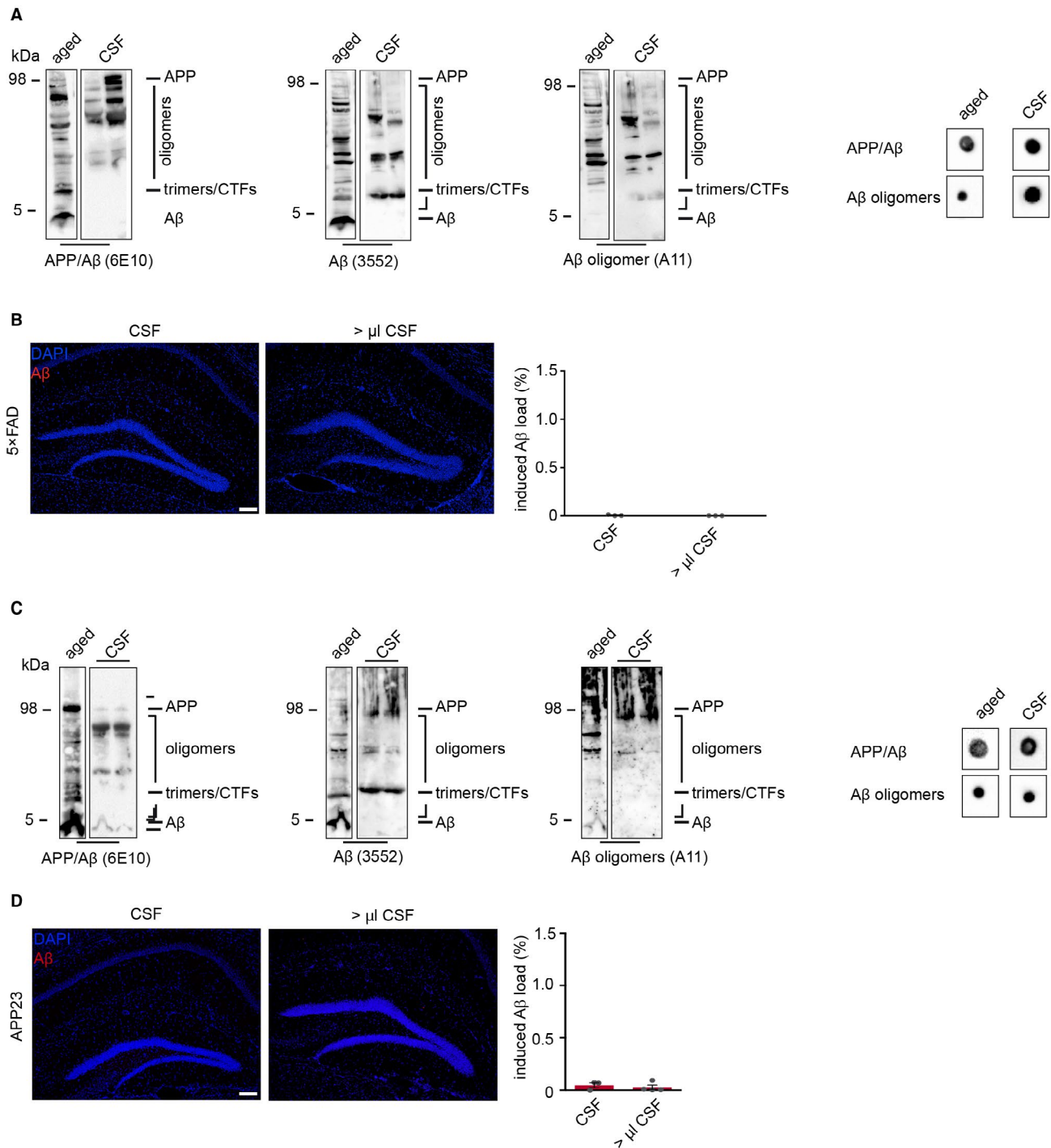


**Figure 3.** Seeding capacity of A $\beta$  oligomers from murine CSF. **A.** CSF from young, 9-week-old 5x FAD mice revealed the presence of A $\beta$  oligomers but no monomeric A $\beta$  that was confirmed by dot blot analysis. **B.** Despite these high levels of oligomeric A $\beta$  in the CSF of young mice, this preparation failed to induce A $\beta$  deposition. **C.** Immunoblot and dot blot analyses confirmed the abundance of oligomeric A $\beta$  in the CSF of 21-week-old APP23 transgenic mice as well (each lane represents a

different CSF probe) when compared to aged brain homogenate. **D.** Undiluted murine CSF from APP23 mice was injected into young, predeposited APP23 transgenic mice and analyzed after a 3-month incubation period. Neither CSF from APP23 mice nor higher volumes of the CSF revealed any seed-induced A $\beta$  depositions. Scale bar in (B, D) indicates 100  $\mu$ m. (B) n(2.5  $\mu$ l CSF) = 3; n(5  $\mu$ l CSF) = 3. (D) n(2.5  $\mu$ l CSF) = 3; n(5  $\mu$ l CSF) = 4. Indicated is the mean  $\pm$  S.E.M.

phase. These results are in agreement with studies demonstrating that polymerization of A $\beta$  aggregates can occur through a secondary pathway that overtakes primary nucleation as the relevant source of new oligomers (2, 18), supporting the notion that A11-reactive oligomers seem to be important in the early initial phase of the seeding process. However, despite the high abundance of A $\beta$  oligomers in the CSF and brain homogenate of young APP transgenic mice, those preparations failed to induce A $\beta$  seeding. Thus, monomeric species of A $\beta$  might be sufficient for the initiation of A $\beta$  plaque formation which is in line with a previous finding by another group showing formaldehyde fixed brain homogenate that contains predominantly monomeric A $\beta$  displayed plenty of seeding capacity (8). Nevertheless, we can't exclude the possibility that there is an as yet "unknown" factor and/or A $\beta$  fibrils in the brain homogenate that is missing in the brain extract of young mice as well as in the CSF. Another study with similar results attributed the lack of N-terminally truncated A $\beta$  species and smaller A $\beta$  particles in the CSF to its failure to induce A $\beta$  seeding (9). Future studies should include a detailed biochemical investigation

of both extracts in comparison to aged brain homogenate. To finally address the question if monomers alone are sufficient to induce A $\beta$  seeding, it will be important to study brain homogenate with significantly reduced monomer content.

*In vitro* experiments showed that oligomer growth follows a defined mechanism that is distinct from fibril growth and independent of the monomer concentration by adding only one monomer at a time (3, 22). Thus, the missing part of preformed oligomers will most likely be replenished by newly generated oligomers, a process that is known to be less dependent on monomer concentration but on time, finally extending the lag phase and shifting the aggregation curve to the right. The fibrils formed afterward by nucleated conformational conversion of A11-reactive oligomers might grow rapidly due to the increased access of A $\beta$  monomers (17). The monomers, as the fundamental building blocks for all subsequent intermediate forms of A $\beta$  peptides in the aggregation process on the way to insoluble mature fibrils and finally to amyloid plaques, should hence be able to form the initial nucleus that is needed for seed-induced A $\beta$  deposition.

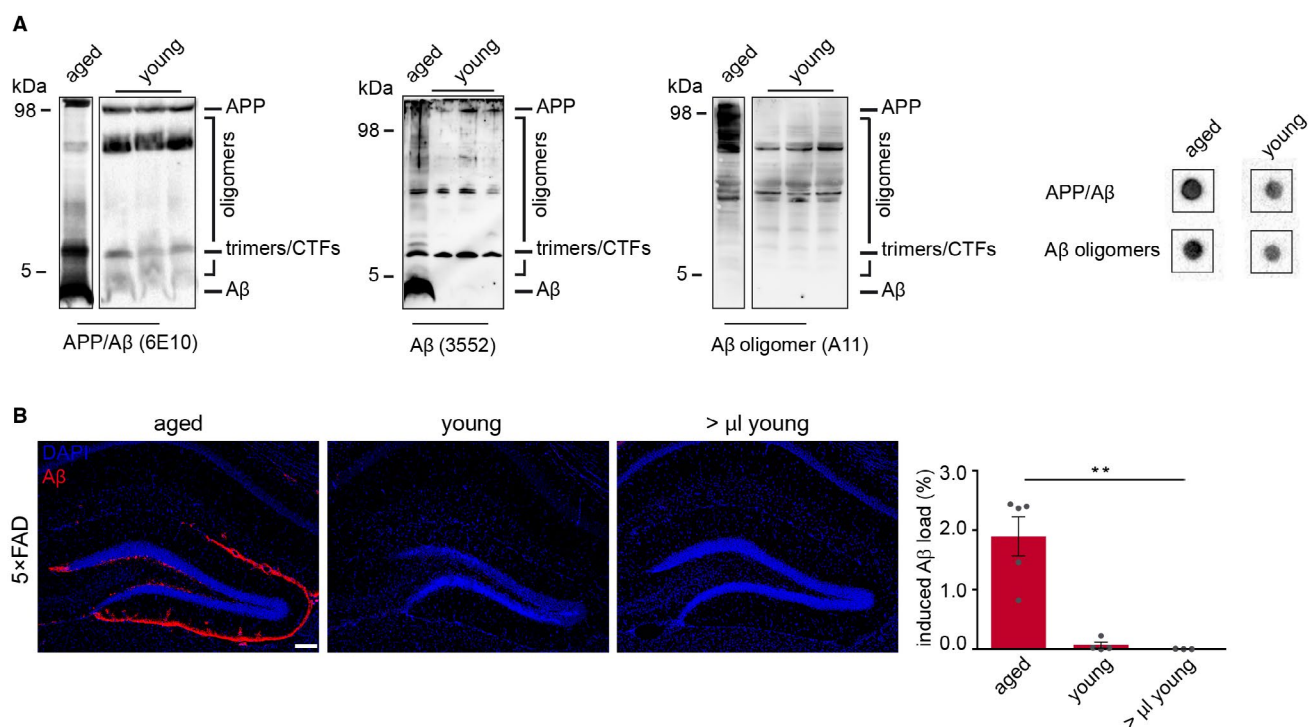


**Figure 4.** Seeding capacity of A $\beta$  oligomers from young 5xFAD mice. **A.** Immunoblot analysis using SDS-PAGE and dot blot assay (right panel) revealed the presence of A $\beta$  oligomers but no monomeric A $\beta$  in brain homogenates of young, 16-week-old 5xFAD transgenic mice. Membranes were probed with hA $\beta$ /APP-specific antibody 6E10, 3552 or A $\beta$  oligomer-specific antibody A11. The presence of A $\beta$  oligomers in young brain homogenate was also confirmed by dot blot analysis. **B.** Immunofluorescence staining against A $\beta$  with antibody 3552 (red)

showed robust induced A $\beta$  deposition when 10% w/v of aged brain homogenate was injected, whereas no amyloid deposition was observed with young brain homogenate even with higher volumes. Scale bar in (B) represents 100  $\mu$ m. One-way ANOVA  $F(2,9) = 21.09$ ;  $P = 0.0004$ ; Bonferroni's multiple comparisons test  $**P < 0.0021$ .  $n(\text{aged brain homogenate}) = 5$ ;  $n(2.5 \mu\text{L young brain homogenate}) = 4$ ;  $n(5.0 \mu\text{L young brain homogenate}) = 3$ . Indicated is the mean  $\pm$  S.E.M.



## ACKNOWLEDGEMENTS

We are particularly grateful to J. Göldner, D. Bleckmann and T. Bachhuber for technical assistance and G. Fritz for advice and discussions.

This work was supported by the Fill in the Gap fellowship (Medical Faculty Freiburg) to N.K., the Emmy Noether Program of the Deutsche Forschungsgemeinschaft (Grant number: ME 3542/1-1 to M.M.L.) and a grant of the Deutsche Forschungsgemeinschaft (Grant number: ME 3542/2-1 to M.M.L.).

## DATA AVAILABILITY STATEMENT

Data sharing is not applicable to this article as no new data were created or analyzed in this study.

## ETHICS APPROVAL

All animal studies were reviewed, approved and carried out in accordance with the policies of the state of Baden-Württemberg under license numbers G13-093 and G16-60.

## AUTHORS CONTRIBUTIONS

N.K. and M.M.-L. conceived and designed the study. N.K. contributed to all aspects of the experiments and data analysis. N.S., S.Z.-W., C.W. and C.A.-A. assisted with the experimental work. B.N. carried out the ELISA experiments. N.K., M.P., C.H. and M.M.-L. discussed the results. M.M.-L. wrote the manuscript with help from N.K. and further input from all co-authors. The APP23 mice were a kind gift of Novartis, Basel, Switzerland. All authors read and approved the final manuscript.

## COMPETING FINANCIAL INTERESTS

C.H. is an advisor of F. Hoffmann-La Roche and has a collaboration agreement with DENALI. All other authors declare that they have no conflict of interest.

## REFERENCES

- Bachhuber T, Katzmarski N, McCarter JF, Loreth D, Tahirovic S, Kamp F *et al* (2015) Inhibition of amyloid-beta plaque formation by alpha-synuclein. *Nat Med* **21**:802–807.
- Cohen SI, Linse S, Luheshi LM, Hellstrand E, White DA, Rajah L *et al* (2013) Proliferation of amyloid-beta42 aggregates occurs through a secondary nucleation mechanism. *Proc Natl Acad Sci U S A* **110**:9758–9763.
- Collins SR, Douglass A, Vale RD, Weissman JS (2004) Mechanism of prion propagation: amyloid growth occurs by monomer addition. *PLoS Biol* **2**:e321.
- DeMattos RB, Bales KR, Parsadanian M, O'Dell MA, Foss EM, Paul SM, Holtzman DM (2002) Plaque-associated disruption of CSF and plasma amyloid-beta (A $\beta$ ) equilibrium in a mouse model of Alzheimer's disease. *J Neurochem* **81**:229–236.
- Duran-Aniotz C, Morales R, Moreno-Gonzalez I, Hu PP, Fedynyshyn J, Soto C (2014) Aggregate-depleted brain fails to induce A $\beta$  deposition in a mouse model of Alzheimer's disease. *PLoS One* **9**:e89014.
- Forný-Germano L, e Silva NM, Batista AF, Brito-Moreira J, Gralle M, Boehnke SE *et al* (2014) Alzheimer's disease-like pathology induced by amyloid-beta oligomers in nonhuman primates. *J Neurosci* **34**:13629–13643.
- Fritsch SK, Cintron A, Ye L, Mahler J, Buhler A, Baumann F *et al* (2014) A $\beta$  seeds resist inactivation by formaldehyde. *Acta Neuropathol* **128**:477–484.
- Fritsch SK, Langer F, Kaeser SA, Maia LF, Portelius E, Pinotsi D *et al* (2014) Highly potent soluble amyloid-beta seeds in human Alzheimer brain but not cerebrospinal fluid. *Brain* **137**(Pt 11):2909–2915.
- Hardy J, Selkoe DJ (2002) The amyloid hypothesis of Alzheimer's disease: progress and problems on the road to therapeutics. *Science* **297**:353–356.
- Jucker M, Walker LC (2013) Self-propagation of pathogenic protein aggregates in neurodegenerative diseases. *Nature* **501**:45–51.
- Kane MD, Lipinski WJ, Callahan MJ, Bian F, Durham RA, Schwarz RD *et al* (2000) Evidence for seeding of beta-amyloid by intracerebral infusion of Alzheimer brain extracts in beta-amyloid precursor protein-transgenic mice. *J Neurosci* **20**:3606–3611.
- Kayed R, Head E, Thompson JL, McIntire TM, Milton SC, Cotman CW, Glabe CG (2003) Common structure of soluble amyloid oligomers implies common mechanism of pathogenesis. *Science* **300**:486–489.
- Koffie RM, Meyer-Luehmann M, Hashimoto T, Adams KW, Mielke ML, Garcia-Alloza M *et al* (2009) Oligomeric amyloid beta associates with postsynaptic densities and correlates with excitatory synapse loss near senile plaques. *Proc Natl Acad Sci U S A* **106**:4012–4017.
- Langer F, Eisele YS, Fritsch SK, Staufenbiel M, Walker LC, Jucker M (2011) Soluble A $\beta$  seeds are potent inducers of cerebral beta-amyloid deposition. *J Neurosci* **31**:14488–14495.
- Lee J, Culyba EK, Powers ET, Kelly JW (2011) Amyloid-beta forms fibrils by nucleated conformational conversion of oligomers. *Nat Chem Biol* **7**:602–609.
- Lee EB, Leng LZ, Zhang B, Kwong L, Trojanowski JQ, Abel T, Lee VM (2006) Targeting amyloid-beta peptide (A $\beta$ ) oligomers by passive immunization with a conformation-selective monoclonal antibody improves learning and memory in A $\beta$  precursor protein (APP) transgenic mice. *J Biol Chem* **281**:4292–4299.
- Liu P, Reed MN, Kotilinek LA, Grant MK, Forster CL, Qiang W *et al* (2015) Quaternary structure defines a large class of amyloid-beta oligomers neutralized by sequestration. *Cell Rep* **11**:1760–1771.
- Maia LF, Kaeser SA, Reichwald J, Hruscha M, Martus P, Staufenbiel M, Jucker M (2013) Changes in amyloid-beta and Tau in the cerebrospinal fluid of transgenic mice overexpressing amyloid precursor protein. *Sci Transl Med* **5**:194re2.
- Meyer-Luehmann M, Coomaraswamy J, Bolmont T, Kaeser S, Schaefer C, Kilger E *et al* (2006) Exogenous induction of cerebral beta-amyloidogenesis is governed by agent and host. *Science* **313**:1781–1784.
- Morales R, Bravo-Alegria J, Duran-Aniotz C, Soto C (2015) Titration of biologically active amyloid-beta seeds in a transgenic mouse model of Alzheimer's disease. *Sci Rep* **5**:9349.

21. Nguyen PH, Li MS, Stock G, Straub JE, Thirumalai D (2007) Monomer adds to preformed structured oligomers of Abeta-peptides by a two-stage dock-lock mechanism. *Proc Natl Acad Sci U S A* **104**:111–116.
22. Oakley H, Cole SL, Logan S, Maus E, Shao P, Craft J *et al* (2006) Intraneuronal beta-amyloid aggregates, neurodegeneration, and neuron loss in transgenic mice with five familial Alzheimer's disease mutations: potential factors in amyloid plaque formation. *J Neurosci* **26**:10129–10140.
23. Page RM, Baumann K, Tomioka M, Perez-Revuelta BI, Fukumori A, Jacobsen H *et al* (2008) Generation of Abeta38 and Abeta42 is independently and differentially affected by familial Alzheimer disease-associated presenilin mutations and gamma-secretase modulation. *J Biol Chem* **283**:677–683.
24. Page RM, Gutsmedl A, Fukumori A, Winkler E, Haass C, Steiner H (2010) Beta-amyloid precursor protein mutants respond to gamma-secretase modulators. *J Biol Chem* **285**:17798–17810.
25. Paxinos GF, KBJ (2001) The Mouse Brain in Stereotaxic Coordinates, 2nd edn. Academic Press: San Diego, CA.
26. Rasool S, Albay R 3rd, Martinez-Coria H, Breydo L, Wu J, Milton S *et al* (2012) Vaccination with a non-human random sequence amyloid oligomer mimic results in improved cognitive function and reduced plaque deposition and micro hemorrhage in Tg2576 mice. *Mol Neurodegener* **7**:37.
27. Rasool S, Martinez-Coria H, Wu JW, LaFerla F, Glabe CG (2013) Systemic vaccination with anti-oligomeric monoclonal antibodies improves cognitive function by reducing Abeta deposition and tau pathology in 3xTg-AD mice. *J Neurochem* **126**:473–482.
28. Stohr J, Watts JC, Mensinger ZL, Oehler A, Grillo SK, DeArmond SJ *et al* (2012) Purified and synthetic Alzheimer's amyloid beta (Abeta) prions. *Proc Natl Acad Sci U S A* **109**:11025–11030.
29. De Strooper B, Karran E (2016) The cellular phase of Alzheimer's disease. *Cell* **164**:603–615.
30. Sturchler-Pierrat C, Abramowski D, Duke M, Wiederhold KH, Mistl C, Rothacher S *et al* (1997) Two amyloid precursor protein transgenic mouse models with Alzheimer disease-like pathology. *Proc Natl Acad Sci U S A* **94**:13287–13292.
31. Walsh DM, Klyubin I, Fadeeva JV, Cullen WK, Anwyl R, Wolfe MS *et al* (2002) Naturally secreted oligomers of amyloid beta protein potently inhibit hippocampal long-term potentiation *in vivo*. *Nature* **416**:535–539.
32. Walsh DM, Selkoe DJ (2007) A beta oligomers—a decade of discovery. *J Neurochem* **101**:1172–1184.
33. Yamasaki A, Eimer S, Okochi M, Smialowska A, Kaether C, Baumeister R *et al* (2006) The GxGD motif of presenilin contributes to catalytic function and substrate identification of gamma-secretase. *J Neurosci* **26**:3821–3828.
34. Yang T, Li S, Xu H, Walsh DM, Selkoe DJ (2017) Large soluble oligomers of amyloid beta-protein from Alzheimer brain are far less neuroactive than the smaller oligomers to which they dissociate. *J Neurosci* **37**:152–163.
35. Ye L, Hamaguchi T, Fritsch SK, Eisele YS, Obermuller U, Jucker M, Walker LC (2015) Progression of seed-induced Abeta deposition within the limbic connectome. *Brain Pathol* **25**:743–752.
36. Ziegler-Waldkirch S, Sauer JF, Erny D, Savanthrapadian S, Loreth D, Katzmarski N *et al* (2018) Seed-induced Abeta deposition is modulated by microglia under environmental enrichment in a mouse model of Alzheimer's disease. *EMBO J* **37**:167–182.

## SUPPORTING INFORMATION

Additional supporting information may be found in the online version of this article at the publisher's web site:

**Figure S1. Induced A $\beta$  deposition.** (A) Fluorescence microscopy of A $\beta$  (red) and DAPI (blue) in 5 $\times$ FAD mice either 6 weeks or (B) 10 weeks post-injection with transgenic brain homogenate, or in uninjected control 5 $\times$ FAD animals at the same age. (C) Fluorescence microscopy of A $\beta$  (red) and DAPI (blue) in APP23 mice 18 weeks post-injection with transgenic brain homogenate or in uninjected control APP23 mice at the same age. Scale bars represent 100  $\mu$ m.

**Figure S2. Formation of dense core plaques after injection of oligomer-depleted brain homogenate.** (A) Thiazine Red staining to detect dense core plaques revealed similar numbers of plaques in the hippocampus (a; insert i and iii) and entorhinal cortex (a; insert ii and iv) of 5 $\times$ FAD mice 10 weeks after injection. Mann-Whitney test: n.s. Scale bar in (A) represents 500  $\mu$ m and in the inserts 100  $\mu$ m. Indicated is the mean  $\pm$  S.E.M per group. (B) The number of dense core plaques within the seeding pattern of the dentate gyrus was not significantly different between both injection groups (complete versus oligomer-depleted brain homogenate; n = 4). Inserts in the middle panel confirmed the existence of dense-core plaques within the seeding area by co-labeling of A $\beta$  plaques (with antibody 3552 in green) and thiazinred. Mann-Whitney test: n.s. Scale bar in (B) represents 100  $\mu$ m. Indicated is the mean  $\pm$  S.E.M per group.

**Figure S3. Impact of A $\beta$  oligomers on neuronal precursor cells.** Fluorescence microscopy of DCX (red) and DAPI (blue) at 2, 8 and 10 weeks post-injection. Quantification of DCX-positive cells in the dentate gyrus of 5 $\times$ FAD transgenic mice either injected with complete homogenate or oligomer-depleted brain homogenate revealed a decrease in DCX positive cells over time, but no significant difference between both injection groups was observed (complete brain homogenate n = 5 for all time points; A $\beta$  oligomer IP: n(2, 10 weeks) = 4; n(8 weeks) = 3; Kruskal-Wallis test \*\*\*0.0004; Dunn's multiple comparisons test). Scale bar represents 100  $\mu$ m and in the inserts 20  $\mu$ m. Indicated is the mean  $\pm$  S.E.M per group.